OXFORD

L_1 regularization facilitates detection of cell type-specific parameters in dynamical systems

Bernhard Steiert[1,*], Jens Timmer[1,2,3] and Clemens Kreutz[1,3]

[1]Institute of Physics, [2]BIOSS Centre for Biological Signalling Studies and [3]Freiburg Center for Systems Biology (ZBSA), University of Freiburg, Germany

*To whom correspondence should be addressed.

Abstract

Motivation: A major goal of drug development is to selectively target certain cell types. Cellular decisions influenced by drugs are often dependent on the dynamic processing of information. Selective responses can be achieved by differences between the involved cell types at levels of receptor, signaling, gene regulation or further downstream. Therefore, a systematic approach to detect and quantify cell type-specific parameters in dynamical systems becomes necessary.

Results: Here, we demonstrate that a combination of nonlinear modeling with L_1 regularization is capable of detecting cell type-specific parameters. To adapt the least-squares numerical optimization routine to L_1 regularization, sub-gradient strategies as well as truncation of proposed optimization steps were implemented. Likelihood-ratio tests were used to determine the optimal regularization strength resulting in a sparse solution in terms of a minimal number of cell type-specific parameters that is in agreement with the data. By applying our implementation to a realistic dynamical benchmark model of the *DREAM6* challenge we were able to recover parameter differences with an accuracy of 78%. Within the subset of detected differences, 91% were in agreement with their true value. Furthermore, we found that the results could be improved using the profile likelihood. In conclusion, the approach constitutes a general method to infer an overarching model with a minimum number of individual parameters for the particular models.

Availability and Implementation: A MATLAB implementation is provided within the freely available, open-source modeling environment Data2Dynamics. Source code for all examples is provided online at http://www.data2dynamics.org/.

Contact: bernhard.steiert@fdm.uni-freiburg.de

1 Introduction

The progress in the development of experimental assays like the establishment of high-throughput measurement techniques raised new demands on statistical methodology. Many scientific questions in the field of Bioinformatics and Systems Biology nowadays require large models with hundreds or even thousands of parameters or variables. Therefore, a major issue in many applications is feature selection, i.e. determination of informative parameters or variables, which are required to explain experimental observations, for identification of differential expression and/or for making reliable predictions.

Selecting parameters of interest is one of the most important tasks during modeling as it heavily influences predictions. In many cases, feature selection is equivalent to model discrimination (Box and Hill, 1967) since a set of features corresponds to a specific model with a corresponding set of parameters. In *multiple linear regression*, as an example, feature selection corresponds to choosing appropriate prediction variables used to fit an experimentally observed response variable. The traditional approach for choosing a suitable level of detail and the respective optimal set of features is iteratively testing many models (Thompson, 1978), i.e. different subsets of features by *forward-* or *backward selection* or combinations thereof (Efroymson, 1960; Hocking and Leslie, 1967). However, if the number of potential predictors is large, the number of possible combinations increases dramatically as shown in Figure 1, rendering such iterative procedures as infeasible.

Regularization techniques have been suggested as an alternative approach for selecting features and fitting parameters in a single step. The idea is to estimate the parameters by optimizing an appropriate objective function, e.g. by maximizing the *likelihood*. If then, in addition, the impact of individual features is penalized, the optimal solution becomes sparse and the level of sparsity can be controlled by the strength of penalization. It has been shown that such penalties are equivalent to utilization of prior knowledge supplemental to the information provided by the data.
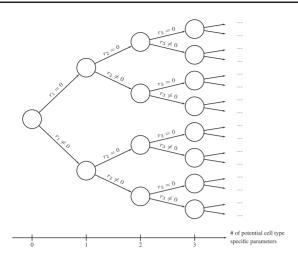
Fig. 1. Naïve approach to select cell type-specific parameters. Each parameter p_i for two cell types could be either cell type-independent or -specific. Then, the log fold-change $r_i = \log_{10}(p_{i,\text{ct2}}/p_{i,\text{ct1}})$ is either $= 0$, or $\neq 0$, respectively. Hence, the number of model candidates (circles) grows exponentially with the number of potential cell type-specific parameters (x-axis)

The additional information provided by penalties reduces the variance of the estimated parameters but at the same time introduces a bias. This effect has been termed as *shrinkage*. If the regularizing penalties are chosen appropriately, e.g. if the L_0- or L_1-norms are applied, a second effect occurs which can be utilized for selection. Because the L_0- and L_1-norms penalize parameters unequal to zero, only parameters remain in the model, which are mandatory for explaining the data. Since the penalized likelihood is discontinuous for L_0 regularization, L_1 penalties are usually preferred.

The concept of using the L_1-norm for data analysis and for calibrating a model has been applied in several fields like for deconvolution of wavelets (Taylor *et al.*, 1979), reconstruction of sparse spike trains of Fourier components (Levy and Fullagar, 1981), recovering acoustic impedance of seismograms (Oldenburg *et al.*, 1983) as well as for *compressed sensing* (Candes and Wakin, 2008; Cheng, 2015) and clinical prediction models (Hothorn and Bühlmann, 2006). Additionally, it has been used to establish statistical methods which are robust against violations of distributional assumptions about measurement errors (Barrodale and Roberts, 1973; Claerbout and Muir, 1973). Moreover, L_1 penalties have been utilized to incorporate *Laplacian priors* (Kabán, 2007). Despite this variety of applications, the usability for feature selection and a comprehensive statistical interpretation was not established until introduction of the *LASSO (least absolute shrinkage and selection operator)*. This prominent approach for linear models was published in Tibshirani (1996) when the first affordable high-throughput techniques were available and the necessity of new approaches for analyzing high-throughput data became inevitable.

The standard *LASSO* has been generalized and adapted specifically in several directions. Feature selection via *LASSO* was discussed for the regression case in more detail in Tibshirani (1996), for Cox-regression in Tibshirani (1997), and for clustering e.g. in Witten and Tibshirani (2010). The *elastic net* has been introduced as a combination of L_1 and L_2 regularization (Zou and Hastie, 2005). The so-called *group-LASSO* has been established to select between predefined groups of features (Ming Yuan, 2006), the *fused LASSO* has been introduced to account for additional constraints of pairs of parameters (Tibshirani *et al.*, 2005), and the *generalized LASSO* has been developed to regularize arbitrary prespecified parameter linear combinations (Tibshirani and Taylor, 2011).

Mechanistic *ordinary differential equation (ODE)* models are applied in Systems Biology for describing and understanding cellular signal transduction pathways, gene regulatory networks, and metabolism. For such ODE models, the selection issue occurs when several cell types are considered. Since each cell type has different concentrations of intracellular compounds and diverse structures, each parameter of a reaction network could potentially be different. We suggest L_1 regularization in this setting to predict parameter differences between cell types. In contrast to the usual context of L_1 regularization, cell type-specific parameters instead of variables are selected. All components of mechanistic models have counterparts in the biological pathway of interest. Therefore, the models are large and the effect of the parameters on the dynamics is typically strongly nonlinear. For estimating parameters in such ODE models, only a small subset of optimization routines in combination with appropriate strategies for calculating derivatives of the objective function, dealing with non-identifiability, handling of local minima etc. are applicable (Raue *et al.*, 2013). We therefore augment an existing and well-tested implementation for parameter estimation for such systems (Raue *et al.*, 2015) to perform selection of cell type-specific parameters based on L_1 regularization. For this purpose, trust-region optimization (Coleman and Li, 1996) was combined with a suitable strategy as presented in Schmidt *et al.* (2009) to enable efficient optimization in the presence of L_1 penalties in nonlinear models.

Since shrinkage, i.e. decreasing the variance by introducing a bias is not intended for mechanistic models, we only use L_1 regularization for selection, i.e. determining the cell type-specific parameters, and then use the resulting *parsimonious model* to estimate the unbiased magnitude of all parameters in a second step. An appropriate strategy for choosing the optimal regularization strength in this setting is presented. The applicability is demonstrated using a benchmark model from the *DREAM (Dialogue for Reverse Engineering Assessment and Methods)* parameter estimation challenge (Meyer *et al.*, 2014). The presented approach constitutes a suitable methodology to infer cell type-specific parameters. In addition, these could be used to predict cell type-specific sensitivities for drugs, which is a prominent challenge in cancer research.

2 Problem statement

Given a model $\mathcal{M}$ describing the kinetics of c reaction network components x_q with $q \in [1, \ldots, c]$ by a system of *ODEs*

$$\dot{x}(t) = f(x(t), u(t, p_u), p_x) \tag{1}$$

with a solution vector $x(t)$ representing concentrations of molecular compounds, for external inputs $u(t)$. States x are mapped to experimental data y using an observation function g, yielding

$$y(t) = g(x(t), p_y) + \epsilon(\sigma(p_\sigma, x(t))). \tag{2}$$

The measurement error $\epsilon \sim \mathcal{N}(0, \sigma^2)$ is assumed to be normally distributed according to an error model $\sigma(p_\sigma, x(t))$, although the presented approach is not limited to this assumption. Initial concentrations p_0, as well as parameters p_x of the ODE, p_u of the input, p_y of the observation function, p_σ of the error model, are subsumed in the parameter vector

$$p = [p_0, p_x, p_u, p_y, p_\sigma]. \tag{3}$$

The expressions (Equations 1–3) fully specify $\mathcal{M}$. To ensure positive values and improve numerical stability, all parameters are log-transformed.

Given data from two cell types can be described by a common ODE structure (Equation 1). Then, in general, the parameters p are specific for each cell type (ct), i.e. $p_{ct1} \neq p_{ct2}$. However, some of the components of p_{ct1} and p_{ct2} may be independent from the cell type. Discovering which of the components in p_{ct1} and p_{ct2} are most likely to be cell type-specific is the main topic of this manuscript. A naïve approach is to simply test all possibilities for cell type-specific parameters. However, as depicted in Figure 1, the number of model candidates grows exponentially with the number of parameters, rendering such an approach as infeasible.

2.1 Unbiased parameter estimation

To estimate parameters p for n data points y_j, given the corresponding observation function observation $g(x(t_j), p_y)$, which is dependent on the ODE solution, the negative 2-fold log-likelihood

$$-2 \log \mathcal{L}(p) = \sum_{j=1}^{n} \frac{(y_j - g(x(t_j), p_y))^2}{\sigma_j^2} =: \chi^2 \qquad (4)$$

is optimized, resulting in the maximum likelihood estimate

$$\widehat{p} = \arg \min \left[\chi^2(p) \right]. \qquad (5)$$

In general, the ODE system cannot be solved analytically. Therefore, numerical methods as implemented in the Data2Dynamics modeling environment (Raue *et al.*, 2015) are used for calculating ODE solutions and performing maximum likelihood estimation. In addition, we employ multi-start deterministic local optimization as an established approach to ensure that $\widehat{p}$ is in fact the global optimum, as presented in Raue *et al.* (2013).

2.2 Regularization

Regularization constitutes a prominent method to incorporate prior knowledge, for parameter selection, or to improve numerics of parameter estimation. Here, we use L_k regularization by a penalty to assess the fold-change $\tilde{r}_i$ of parameters between cell type 1 and cell type 2, i.e. $p_{i,ct2} = \tilde{r}_i \cdot p_{i,ct1}$. Therefore, the penalized likelihood

$$\chi_{L_k}^2(p, r) = \chi^2(p) + \lambda \left(\sum_i |\log \tilde{r}_i|^k \right)^{1/k} \qquad (6)$$

is implemented consisting of the likelihood (Equation 4) and a L_k regularization term weighted by λ. In the following, we substitute $r_i := \log \tilde{r}_i$. The regularization term corresponds to a prior in a Bayesian framework: e.g. for $k = 1$ the L_1 prior is a Laplacian function, and for $k = 2$ the L_2 prior is a Gaussian function. Using the definition

$$||r||_k := \left(\sum_i |r_i|^k \right)^{1/k} \qquad (7)$$

of a L_k-norm, we derive properties of L_k for ranges of $k \in \mathbb{R}^+$, similar to Vidaurre *et al.* (2013). L_0 is the apparent choice for parameter selection due to its direct penalization of the number of $r_i \neq 0$. However, L_0 is not recommended because the associated optimization problem is known to be NP-hard, i.e. the exact solution cannot be obtained within polynomial computation time. In general, for $k < 1$, the L_k metric is non-convex which severely hampers numerical methods for parameter estimation. On the positive side, $k \leq 1$, for example L_0 and L_1, induces sparsity with the results usually being similar. In contrast, the L_k metric for $k > 1$ does not lead to sparse results. L_2, which is the metric used for the well-known least squares, can be handled efficiently but does not produce sparse

results without introducing heuristics. In that sense, the L_1 metric is unique because it is the only one that combines both features, convexity and sparsity. Therefore, L_1 is the natural choice for parameter selection and is used in the following.

Figure 2 demonstrates how sparsity is induced by the L_1-norm. In the upper row, the data contribution (χ^2) is depicted by the solid black line, representing a hypothetical model. The L_1 contribution is shown by the dashed blue line. With increasing λ from panels left to right, the influence of the L_1 term is increased. The lower row shows the penalized likelihood (Equation 6) for $k = 1$, i.e. the sum of the two lines in the corresponding upper panel. For $\lambda = 0.5$, the minimum is shifted towards zero (middle panel) in contrast to the unregularized minimum (left panel) but still different from zero. In contrast, the minimum is exactly at zero for $\lambda = 2$ (right panel).

2.3 Regularized parameter estimation

Optimization in context of partially observed nonlinear coupled ODEs is challenging. However, methods have been developed to efficiently compute solutions of this problem (Raue *et al.*, 2013). To augment the existing implementations with L_1 regularization, i.e. to minimize the penalized likelihood

$$\chi_{L_1}^2(p, r, \lambda) = \chi^2(p) + \lambda \sum_i |r_i| \qquad (8)$$

the adaptations described in the following were implemented. Efficient optimization routines like Gauss-Newton or Levenberg-Marquardt exploit the quadratic form in Equation (4). For example, the implementation of a trust-region method *lsqnonlin* in MATLAB requires residuals

$$\text{res}_j = \frac{y_j - g(x(t_j), p_y)}{\sigma_j} \qquad (9)$$

for data points y_j as input and implicitly calculates the value of the objective function by summation over squares of all residuals. To enable optimization of the penalized likelihood (Equation 8),

$$\text{res}_i = \sqrt{\frac{|r_i|}{1/\lambda}} \qquad (10)$$

is appended to the residuals vector for each fold-change r_i. The associated sensitivities
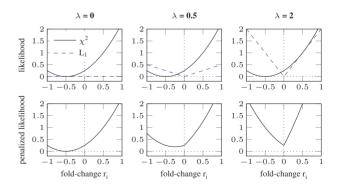

Fig. 2. Sparsity and bias introduced by L_1 regularization. Regularization weight λ is increased from panels left to right. In the upper row, the contributions from the data (χ^2—black line) and a L_1 regularization term (dashed blue line) are shown. Their sum is plotted in the lower row. For $\lambda = 0.5$, a bias is introduced shifting the minimum towards zero (middle column). When λ is increased to 2, the minimum is exactly at zero, i.e. sparsity is induced (right column)

$$\mathrm{sres}_{ij} := \frac{\partial \mathrm{res}_j}{\partial p_i} \qquad (11)$$

to the regularization residuals res_i are calculated as

$$\mathrm{sres}_{ii} = \frac{\mathrm{sgn}(r_i)}{\frac{2}{\lambda} \sqrt{\frac{|r_i|}{1/\lambda}}}. \qquad (12)$$

The gradient components

$$\nabla_{r_i} \chi^2_{L_1} = 2\, \mathrm{res}_i \cdot \mathrm{sres}_{ii} = \pm\lambda \qquad (13)$$

coincide with the slope $\pm\lambda$ induced by the L_1 term. For $r_i = 0$, Equation (12) is not defined. In this case, the convergence criterion

$$(\widehat{p}, \widehat{r}) = \arg\max_{(p,r)} \chi^2_{L_1}(p, r, \lambda) \qquad (14)$$

$$\iff \begin{cases} \nabla_{p_i} \chi^2 = 0, & \forall i \\ \nabla_{r_i} \chi^2 + \lambda\, \mathrm{sign}(\widehat{r}_i) = 0, & \text{for } |\widehat{r}_i| > 0 \\ |\nabla_{r_i} \chi^2| \leq \lambda, & \text{for } \widehat{r}_i = 0 \end{cases} \qquad (15)$$

is implemented for $r_i = 0$ by setting

$$\begin{cases} \mathrm{sres}_{ii} = 0, & \text{for } |\nabla_i \chi^2(r_i)| > \lambda \\ \mathrm{sres}_{ij} = 0\; \forall j, & \text{for } |\nabla_i \chi^2(r_i)| \leq \lambda. \end{cases} \qquad (16)$$

The rationale behind Equation (15) is that in addition to the classical optimization criterion of vanishing gradient, the L_1 gradient either compensates the data gradient, or the L_1 contribution dominates the data gradient and constrains the estimate to its center $\widehat{r}_i = 0$. During optimization, this parameter-wise convergence criterion is checked for each candidate r_i at every optimization step. If the latter criterion is fulfilled, the derivative of each residual res_j with respect to r_i is set to zero, i.e. $\mathrm{sres}_{ij} = 0\,\forall j$. Thereby, r_i is fixed to zero for the next iteration step. If at a certain optimization step, the convergence criterion is violated, only the ith L_1 contribution to the gradient is set to zero. This in turn enables r_i that were zero to be released during optimization if there is enough evidence in the data. Both options are formulated in Equation (16).

The L_1 metric has a discontinuous derivative at zero. Therefore, the optimization routine encounters sudden jumps of the derivatives as the sign of r_i changes. For n parameters, there exist 2^n combinations of signs. These hyper-quadrants are called orthants. For an efficient optimization, proposed optimization steps from one orthant to another have to be avoided. There are several methods that cope with this problem. They have in common that they split a proposed optimization step into two: first a step towards zero, then potentially a step away from zero. Their major difference is the strategy how zero-values are achieved. To mimic most of the original behavior of trust-region based methods, we implemented the truncation, i.e. scaling, of an optimization step such that the orthant is maintained. Both convergence and truncation are depicted in Figure 3.

2.4 Regularization strength λ

To choose the optimal value λ^* of the regularization strength, λ is scanned from low to high values and the unregularized likelihood is re-optimized until the mismatch between model and data is too large to accept the associated simplification. Thus, likelihood-ratio statistics are employed to discover admissible values. For L_1 based parameter selection, cross validation has been suggested as an alternative approach to choose the final value for the regularization weight λ. However, for nonlinear models, leaving data out could produce non-identifiabilities and the effect on the prediction error
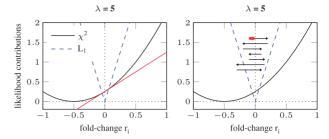

Fig. 3. Convergence criterion and truncation for an optimum of $\chi^2_{L_1}$ at zero. Left panel: the implementation considers a L_1 regularized parameter $r_i = 0$ to be converged if the gradient from the data (χ^2—black line) is smaller than the slope of the L_1 term (dashed blue line). For $r_i = 0$, the algorithm compares the red line, which is the slope of the black line at this point, to the blue dashed line. In this example, the slope of the L_1 term is larger than that of the χ^2 term, hence the minimum is at zero and the corresponding entries in the sensitivity matrix are set to zero. Right panel: The black arrows from top to bottom give a cartoonish representation of optimization steps. To avoid jumping back and forth, i.e. numerical instability by changing the sign of r_i due to discontinuously changing slope of L_1, optimization steps are truncated to the boundary of the orthant as indicated by the red arrow

can be ambiguous. Therefore, we decided to use an information theory based test criterion. The most prominent methods are the likelihood ratio test (LRT; Wilks, 1938), the Akaike information criterion (AIC; Akaike, 1974) and the Bayesian information criterion (BIC; Schwarz, 1978). In certain settings these are equivalent: AIC resembles LRT for fixed $\alpha = 15.6\%$ and one degree of freedom. Further, AIC is known to select systematically too large models and is thus not a consistent model selection criterion, especially for many data points. BIC considers the number of data points and is a consistent model selection criterion. Moreover, BIC is equivalent to LRT with an adjusted α level. Therefore, we only use the LRT in the following without loss of generality.

For certain values of λ, each r_i is estimated either to zero or nonzero by optimizing Equation (8). Then, using Equation (4) the unbiased maximum likelihood estimate is calculated, under the constraint that fold-changes with $\widehat{r}_i = 0$ are fixed to zero. The value of the objective function for this constrained but unbiased solution is denoted as χ^2_λ. The LRT statistic

$$D(\lambda) = \chi^2_\lambda - \chi^2_{\lambda=0} \qquad (17)$$

quantifies the discrepancy to the full model with solely cell type-specific parameters. The cut-off for determining the *parsimonious model*, i.e. the model with a minimal number of differences for a given α level which allows fitting the data, is given by the $\chi^2_{m_\lambda, \alpha}$ distribution with degrees of freedom $m_\lambda = \#r_i - \#(\widehat{r}_i = 0)_\lambda$. Thus, the *parsimonious model* is given by

$$\lambda^* = \max \lambda \;\; \text{s.t.} \;\; D(\lambda) < \chi^2_{m_\lambda, \alpha} \qquad (18)$$

We use the significance level $\alpha = 0.05$ in the following.

2.5 Profile likelihood

The *profile likelihood (PL)* constitutes a method to calculate confidence intervals (CI) of parameters or predictions, see Raue *et al.* (2009) and Kreutz *et al.* (2012) for an overview. It only requires weak assumptions and therefore performs well even for strongly nonlinear problems where asymptotic methods based on the Fisher Information matrix fail. The basic idea is to fix a certain model quantity of interest, e.g. a parameter, and re-optimize all remaining parameters. This re-optimization procedure is iterated for different

fixed values of the quantity of interest. By comparing the increase in χ^2 with respect to the maximum likelihood the CI is calculated.

Here, we use the *PL* to check the parameter differences discovered by our L_1 based implementation. Thus, the unregularized *PL* of a fold-change parameter r_i that has been proposed using L_1 regularization is calculated. If selection was successful, the *PL* should not be compatible with zero. This interpretation is equivalent to a likelihood ratio test between the null model $r_i = 0$ and the alternative model $r_i \neq 0$. Note that we did not use the *PL* in the first place, as the combinatorial issue shown in Figure 1 is not solved by this approach.

In addition, the *PL* can be used to investigate the uniqueness of the solution. In a non-unique setting there are multiple alternatives to select parameter differences. For instance, a selected cell type-specific parameter could be exchanged with another parameter that was not selected as different. For testing uniqueness, the *PL* for each r_i with estimate $\hat{r}_i = 0$ is calculated. This is equivalent to testing a model with one additional free parameter (r_i) in comparison to the *parsimonious model* ($\hat{r}_i \equiv 0$). If inside the CI of r_i, another parameter that was originally different to zero is then compatible with zero, one cannot decide, based on the given data, which one is different. To resolve such an ambiguity, either additional experimental data needs to be collected, or the biologically more reasonable solution could be chosen.

3 Approach

The approach presented in this manuscript extends the available methodology as implemented in the Data2Dynamics modeling environment (Raue *et al.*, 2015) by L_1 regularization. Data2Dynamics is a state-of-the-art software package that has been used in a variety of applications (Bachmann *et al.*, 2011; Becker *et al.*, 2010; Beer *et al.*, 2014) to perform parameter estimation, uncertainty analysis, and experimental design of partially observed nonlinear ODE systems. In the following, we summarize the L_1 specific enhancements in addition to the established modeling routine as implemented in our approach for discovering cell type-specific parameters.

Given an overarching model that is able to describe two cell types with two independent parameter vectors p_{ct1} and p_{ct2} for cell types 1 and 2, respectively. Fold-changes r_i are calculated to express the parameters of cell type 2 relative to cell type 1, i.e. $p_{i,ct2} = \tilde{r}_i \cdot p_{i,ct1}$. Equation (8) is used to L_1 penalize deviations of the fold-change parameter vector r to zero. In contrast to many other *LASSO*-like techniques, our method consists of two consecutive steps:

(i) Determination of cell type-specific parameters using the regularized $\chi^2_{L_1}$
(ii) Determination of the *parsimonious model* and parameter estimates using the unregularized χ^2

In the first step, λ is scanned and the cell type-specific parameters are determined for each value of λ. Then, in the second step, for choosing the optimal λ^* the unregularized Equation (4) is optimized, under the constraint that parameters with $\hat{r}_i = 0$ are shared between both cell types. The full model with all parameters specific for each cell type is compared by the likelihood ratio test to each of the models that were selected using L_1 regularization. Thereby, the *parsimonious model* is defined as the minimal unbiased model that cannot be rejected by the likelihood ratio test.

To cope with diverging terms in the Hessian matrix, we implemented a heuristic that tests each L_1 parameter r_i against zero in the order of their magnitude of deviation from zero. If the likelihood did not increase by more than one, the correction was accepted. Potential alternatives to such a strategy are provided in the discussion.

Additionally, the *PL* can be utilized to further reduce the number of cell type-specific parameters, which we illustrate exemplarily. Further, we show investigation of uniqueness using the *PL*. However, since the calculation of profiles for each parameter and λ can take up to several hours for each of the $N = 500$ runs, these steps were not included for performance assessment of L_1 regularization. When applied in practice, usually only a single experimental setup is analyzed. Then, results can be further improved by calculation of the *PL* pointing out even smaller and/or biologically more plausible solutions.

4 Application

4.1 Model description

In the following, we use model *M1* from the *DREAM6 (Dialogue for Reverse Engineering Assessment and Methods)* challenge as benchmark for our approach (Steiert *et al.*, 2012). The model represents a gene-regulatory network and was chosen because it enables testing many observation setups and parameter differences. It was used in 2011 to evaluate the performance of experimental design strategies to optimize parameters and predictions. The model incorporates transcription and translation of six genes. Therefore, the dynamic variables represent six mRNAs, as well as the six associated proteins with known initial concentrations. Genes can positively and/or negatively regulate each other. Taken together, the model consists of 29 kinetic parameters. 13 are associated with synthesis and degradation of molecules: 1 protein degradation rate which is shared among all proteins; 6 ribosomal strengths determining the synthesis rate of mRNAs; 6 protein synthesis strengths which define how strongly mRNA presence induces protein production. The remaining 16 parameters define the interaction of genes by Hill kinetics, thus 8 K_D values and 8 Hill coefficients are assumed.

DREAM6 M1 was simulated with gold-standard parameters that were made publicly available after completion of the challenge. We used this gold-standard as cell type 1. When complete data is provided, i.e. all observables measured at all possible experimental conditions, all parameters are identifiable, except for one Hill coefficient which is only restricted to lower values. Thus, we conclude that determining parameter differences between cell types is possible in principle. Next, we assumed one third of all parameters to be cell type-specific. We therefore randomly simulated fold-changes $r \in \{1 /10, 1/5, 1/2, 2, 5, 10\}$ for non-Hill parameters. For Hill coefficients, fold changes $r \in \{1/4, 1/2, 2, 4\}$ were assumed such that Hill coefficients are within the interval $[1, 4]$ for both cell types. This range is motivated biologically as thereby the number of binding sites on a molecule is considered. Taken together, the number of possible models is 2^{29}, i.e. more than 10^8.

We chose the following two observation types from the original *DREAM6* challenge setup: (i) mRNA measurements for all mRNAs with 21 data points each, and (ii) protein measurements for two selected proteins, each with 41 data points. The observation function is the identity, i.e. the molecular compounds are observed directly without scaling or offset parameters. The error model contains an absolute term as well as a relative term with fixed weighting. In addition to wild type data, there is the option of performing three possible perturbations for each of the six nodes:

(i) knock-out (mRNA_syn$_i$ = Prot_syn$_i$ = 0)

    (ii) knock-down (mRNA_deg$_i$ → 5 · mRNA_deg$_i$)
    (iii) over-expression (mRNA_syn$_i$ → 2 · mRNA_syn$_i$)

    In total, this results in 18 possible experimental conditions. Wild type data, i.e. mRNA and protein data for all observables, was included for parameter estimation to have a reference for perturbations. Within the challenge, an identifiable setting has been achieved using 9 additional data sets out of 331 possibilities. To allow variability in the number of experiments, we randomly (50%) selected for each of the 18 conditions whether it was observed or not. To mimic the partial observation, which was one task of the *DREAM6* challenge, we chose randomly whether mRNA (one-third) or proteins (two-third) were observed for a given condition. Given the latter, two out of six proteins were randomly selected. We chose the same experimental conditions and observables for both cell types.

    After implementing the fold-changes between cell types, as well as perturbations and observations, we used a L_1 regularization for all fold-change parameters and scanned along λ for parameter selection. To choose the optimal regularization strength λ^* we used the unregularized χ^2. Thus, we could select the *parsimonious model* and ensure unbiased estimates of the fold-change parameters.

4.2 Performance assessment

The procedure of selecting fold-changes and observations was repeated $N = 500$ times, representing 500 different cell type comparison studies. Afterwards, the presented algorithm for L_1 regularized parameter selection was applied in an unsupervised manner for each data setting. The performance is summarized in Figure 4. For each run, a receiver operating characteristic (ROC) curve is calculated by scanning λ from 10^{-4} to 10^6. The black line depicts the arithmetic mean ROC curve and the shading the standard deviation over all $N = 500$ repetitions. For each of these, the blue dot shows the *parsimonious model* selected by the likelihood-ratio test. Usually, for a given ROC curve the selection criterion is chosen to maximize both sensitivity and specificity simultaneously, which is the point on the ROC curve closest to the upper left corner. Because the blue dots appear centered around this 'kink', we consider the LRT based selection criterion appropriate. On average, the implementation results
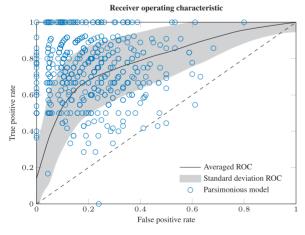
in an around 74% true positive rate (TPR) and an around 20% false positive rate (FPR) for the given setting. The overall accuracy (ACC) is around 78%. Despite this imperfect accuracy and related classification errors, 91% out of the inferred differences, and 93% out of the true positives were estimated closest to their true fold-change. Within the subset of parameters that were modified and afterwards detected as different, 99.5% had the correct sign. Thus, we conclude that the strategy to calculate unbiased estimates for selected fold-changes is robust against misclassification.

    We further evaluated the performance of our L_1 fold-change detection routine for different parameter types. The results are summarized in Table 1. The protein degradation rate is shared among all proteins. It is detected in 100% as different when there was a difference simulated. On the other hand, this parameter also had the highest FPR with approximately 46%. A possible explanation is given by the fact that our method is data driven and hence differences are more likely to be detected in points of the network with more data available. This is the case for the protein degradation rate because it influences all proteins in the network. The individual mRNA and protein synthesis strengths have a FPR around 20% and a TPR of approximately 80%. In contrast, Hill regulation parameters (K_D and Hill coefficient) are detected less frequently as different. This is due to identifiability issues as K_D values and Hill coefficients are only identifiable if the corresponding regulator is in the concentration range around K_D, which is often only given for a small subset of perturbations.

4.3 Supervised examination

In the following, we select one representative setup out of the $N = 500$ given by a minimal deviation of its ROC curve to the average ROC curve for supervised examination. The regularization path is plotted in the left panel of Figure 5. With increasing λ, fold-change parameters are shrinked towards zero, and at some point eventually estimated equal to zero. Thus, the number of cell type-specific parameters decreases for larger λ. The dependency of the likelihood ratio $D(\lambda)$, i.e. the decrease of the unregularized χ^2_λ compared with the full model with only cell type-specific parameters, is shown by the blue line in the right panel of Figure 5. The statistical threshold $\chi^2_{m_\lambda,0.05}$ is depicted by the dashed red line. The regularization strength λ^* at which both lines cross marks the *parsimonious model* that has minimal complexity but cannot be statistically rejected.

Receiver operating characteristic

Fig. 4. Averaged ROC curve. For each of the $N = 500$ runs, the ROC curve is calculated in dependence of λ. The black line depicts the arithmetic mean ROC curve and the shading the standard deviation. Blue circles denote the selected model for each repetition. Because the dots appear on average near the maximum of sensitivity and specificity (upper left corner), we consider the LRT based selection criterion as appropriate. The points $(0, 0)$ and $(1, 1)$ are the limiting cases of no and all, respectively, parameters cell type-specific

Table 1. Performance of algorithm for *DREAM6 M1*

Parameter class	N_{test}	N_{mod}	FPR	TPR	ACC
Protein degradation rate	500	181	0.4577	1.0000	0.7080
mRNA synthesis strength	3000	1032	0.2393	0.7965	0.7730
Protein synthesis strength	3000	986	0.1927	0.7982	0.8043
K_D value	4000	1365	0.1624	0.6989	0.7903
Hill coefficient	4000	1311	0.1852	0.6461	0.7595
All	14 500	4875	0.2006	0.7366	0.7783

On average, one-third of the parameters that could potentially be cell type-specific (N_{test}) were drawn to actually be cell type-specific (N_{mod}). Overall, parameter differences are inferred with 78% ACC. The model contains a shared degradation rate for all proteins, which is often diagnosed as different. Protein production and ribosomal strengths are on average for FPR and TPR. K_D and Hill coefficients are difficult to detect because the concentration range around K_D has to be covered to see an effect on the dynamics. 500 repetitions were computed. Each run, i.e. L_1 regularized scan and subsequent unregularized scan to identify the *parsimonious model*, took 28.8 min on average on an Intel Xeon E5-1620 3.60 GHz desktop computer.
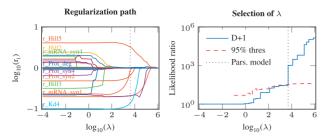
Fig. 5. Left: Regularization path of a representative setup. On the x-axis, the regularization weight λ is depicted. As λ is increased, the number of fold-change parameters unequal to zero is reduced and the estimates are shrinked towards zero. The labels are not exhaustive. As expected for nonlinear models, the individual paths are not necessarily monotonous. The vertical dashed line depicts the *parsimonious* model. Right: Selection of λ. The likelihood-ratio test statistic D is calculated for each value of λ (blue solid line). The value where D crosses the statistical threshold $\chi^2_{m;0.05}$ (dashed red line) marks the *parsimonious model* (dotted black line). To allow plotting in log-space, one is added to all quantities

We checked by calculating the *PL* of the unregularized fold-change parameters whether parameters predicted as cell type-specific are indeed not compatible with zero (Fig. 6). False positive fold change parameters are shown in panels A, D and F. When the *PL* (black line) crosses zero (black vertical dashed line) below the statistical threshold (red horizontal dashed line), the parameter is a candidate for supervised removal. Here, this procedure enables the detection of three additional parameters that could be independent from cell type. Interestingly, all these were false positives. In comparison to the automatically inferred parameter differences, the result of the supervised examination increased the ACC from 79 to 86%. We elaborate more detailed on the origins and consequences of this observation in the discussion.

Further, we checked uniqueness of the solution as shown in Figure 7. The unregularized *PL* of fold-change parameters r_i that were estimated to zero (gray asterisk) is calculated (upper row, black line). Inside the 95%-CI, which is defined by the x-interval for which the *PL* (black line) is below the statistical threshold (red horizontal dashed line), the value of the remaining fold-change parameters r_i is observed (lower row). Then, two scenarios may occur:

i.   none of the r_i is estimated to zero
ii. one or more r_i is estimated to zero

For the *PL* and CI shown in the upper left panel, the re-optimized parameters r_i in the lower panel are not compatible with zero. This corresponds to the first scenario. In contrast, as depicted in the right panels, another fold-change parameter r_i (here: r_Hill8) may be compatible with zero (circle) if the parameter shown on the x-axis (r_mRNA_syn4) is allowed to deviate from zero. This corresponds to the second scenario. Therefore, based on the data, it is not possible to decide which of these two parameters is in fact cell type-specific and which one is independent from cell type. Interestingly, the underlying truth (r_Hill8 $= 0$ and r_mRNA_syn4 $\neq 0$) is contrary to the originally selected difference (r_Hill8 $\neq 0$ and r_mRNA_syn4 $= 0$). Thus, although the *PL* cannot provide which solution is correct it enables to generate alternative hypotheses that are in statistical agreement with the data. Using these hypotheses, experiments could be designed as described in Steiert *et al.* (2012) to eventually obtain an unique solution.

Due to the presented benefits and additional insights, we advise a supervised examination of the results in a real world application to maximize the performance of the method.
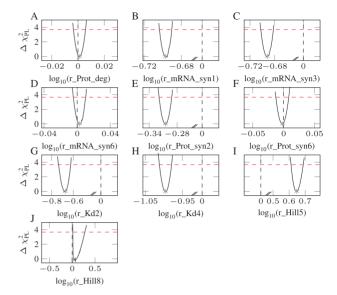

Fig. 6. Determining fold-changes that are compatible with zero (dashed black vertical line) using the *PL*. The parameters in panels B, C, E, G, H, I and J are significantly different from zero, whereas the parameters in panels A, D and F are compatible with zero. These latter ones are actually false positives that could be transformed into true negatives by this supervised examination. Two small diagonal lines depict a discontinuous x-axis
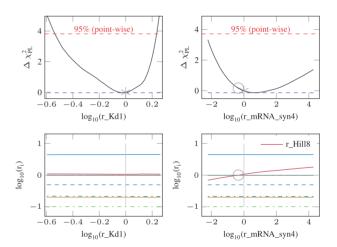

Fig. 7. Uniqueness and exchangeability. The results of the supervised examination example are shown. We used the *PL* to check whether ($r_i = 0$ and $r_j \neq 0$) gives equivalent results as ($r_i \neq 0$ and $r_j = 0$) for $i \neq j$. In the upper row, the *PL* of a fold-change parameter that was estimated to zero is shown. The optimum (asterisk) may not be exactly at the minimum because the model has one additional degree of freedom over the *parsimonious model*. On the lower row, the respective values of the other $\{r_i\}$ are shown. When along the profiled parameter (x-axis), a parameter that was originally non-zero (y-axis) is compatible with zero, it is marked with a circle. On the left hand side, the fold-change parameter r_Kd1, which is a true negative, cannot be exchanged with any other parameter. However, on the right hand side, a false negative fold-change r_mRNA_syn4 could be exchanged with the false positive Hill coefficient r_Hill8. Thus although the solution is incorrect in classifying these two parameters, the *PL* pinpoints the alternative of the correct solution. Given the available data, both cases cannot be distinguished and experimental design would be necessary to decide which one of the parameters is cell type-specific

5 Discussion

In this manuscript, we used L_1 regularization to predict cell type-specific parameters in systems of coupled partially observed ODEs. When compared with the classical *LASSO*, which was designed for

linear models, many pitfalls emerge for parameter estimation in nonlinear ODE systems. Therefore, we augmented an available implementation by L_1 peculiarities and thereby focused on optimization routines that can efficiently handle nonlinearity. Conversely, the popular *LARS* algorithm (Efron *et al.*, 2004) sequentially adds predictors to the model, which is not likely to produce a globally optimal solution in the nonlinear setting. Further, pathwise coordinate optimization (Friedman *et al.*, 2007) exploits that a linear model can be efficiently evaluated, while solving the ODE system is the major bottleneck in our application. Although we cannot completely exclude that the presented methodology may be improved in terms of numerical performance by concepts presented in the vast amount of literature on extending *LASSO*, we could implement a robust and numerically stable algorithm. In our example, cell type-specific parameters were reliably predicted for 500 different data setups.

Because model predictions nonlinearly depend on parameters, the regularization paths depicting the dependency of the cell specific parameters on the regularization strength are not linear between knots. Therefore the regularization paths have to be calculated by discretely scanning λ instead of calculating the paths for whole intervals as it is feasible for linear systems.

Local optima are of major concern in partially observed nonlinear ODE systems. An established method to discover local optima is to perform multi-start deterministic optimization and compare the results. For different λ, other local optima could become globally optimal or even new, additional optima could emerge for a specific range of λ. To circumvent such issues, the multi-start optimization could be applied for each value of λ. However, comprehensively sampling the parameter space by such a strategy is usually computationally infeasible for most realistic models. Therefore, the approach we applied is finding the global optimum for each cell type individually and then gradually increasing λ using the previous fit as initial guess.

Identified differences between cell types may not be unique, i.e. a difference could be exchanged with a parameter that is cell type-independent without significantly changing the fit. Only subgroups of such coupled parameters are necessary to be different. However, this ambiguity is not a shortcoming of the L_1 regularization but rather a manifestation of lacking informative data to uniquely determine cell type-specific parameters.

Most nonlinear optimization algorithms efficiently handle least squares problems but have shortcomings for L_1 regularized optimization. A key challenge that we faced was that numerics became problematic for parameters in the vicinity of zero. For Gauss-Newton steps, the Hessian

$$H_{ij} \approx \text{sres}_{ii} \cdot \text{sres}_{jj} = \frac{\text{sgn}(r_i)}{\frac{2}{\lambda}\sqrt{\frac{|r_i|}{1/\lambda}}} \cdot \frac{\text{sgn}(r_j)}{\frac{2}{\lambda}\sqrt{\frac{|r_j|}{1/\lambda}}}. \tag{19}$$

is approximated by the first-order derivatives sres_{ii}. In this case, r_i appears in the denominator. Therefore, as r_i approaches zero, the Hessian

$$\lim_{r_i \to 0} H_{ij} = \lim_{r_j \to 0} H_{ij} = \pm\infty \tag{20}$$

diverges. For large entries in the Hessian, the optimizer decreases the step size and therefore may get stuck when approaching zero. Thereby, the FPR is increased since parameters compatible with zero shrink but may not be able to actually reach zero. We conclude that the FPR could be further improved if such numerical issues

were completely solved. To overcome these limitations, norms with $k > 1$ could be employed. Although in the proximity of zero L_1 dominates the Hessian, an additional L_2 term like in the *elastic net* could provide enough directional information to come closer to zero. We postpone this analysis to future research.

Another remaining open question is to which extent cross-validation strategies are applicable in the Systems Biology setting. A basic assumption for cross-validation is that the drawn subsets contain qualitatively the same information than the original, full data set. This assumption, however, is violated for pathway models and manifests in a strong dependency of parameter identifiability on resampled data and the experimental setup. The latter originates from the complex grouping structure of measurements given by common treatment conditions, jointly observed dynamic states, as well as by available sampling times.

We chose a benchmark model from the *DREAM6* parameter estimation challenge to demonstrate applicability of our implementation because it provides a variety of predefined realistic experimental setups. For assessing the performance, cell type dependencies of parameters were introduced and then recovered in an unsupervised manner. When compared with typical pathway models, the *DREAM6* setting exhibits two major simplifications. First, the components of the reaction network are directly observed, i.e. there are no scaling parameters. Second, the initial concentrations were assumed as known. However, we do not expect issues if both simplifications are relaxed because the unregularized parameter estimation implementation is well-tested for such cases.

In partially observed nonlinear ODE systems, it has been shown that non-identifiability is of major concern. A non-identifiable parameter can be associated with a flat *PL*, i.e. the effect on observed quantities by changing one parameter can be compensated by others. If the range of a fold-change parameter is compatible with zero, the L_1 regularization will force the estimate to zero. Hence, the presence of non-identifiabilities may decrease the TPR. One example for such a behavior are Hill kinetics, i.e. Hill coefficients and K_D values, which also appeared as most difficult to detect. We conclude that identifiability is limiting the TPR in this setting. Since the subset of available data sets was randomly drawn from the predefined set of experiments, it is not expected that all subsets contain comprehensive information for estimating all parameters. Therefore, identifiability issues naturally occur and appear as false negatives in the parameter selection step. In general, the magnitude of both, correct and incorrect predictions depends on the amount and quality of data, as well as on the size of the underlying differences.

It has to be stated that cell type differences are detected only if there is evidence in the data. Therefore, unobserved components and specific, incomplete measurement conditions increase the chance of missing biologically relevant cell-specific characteristics. However, we could show that the unbiased estimates of true positive fold-changes are robust to misclassification of others. Nevertheless, the final model should always be checked for biological completeness and plausibility.

In summary, we demonstrated the usage of L_1 regularization in combination with nonlinear models based on *ODE* systems. Theoretical considerations were given and the approach was tested for random designs of a *DREAM* benchmark model. The ability to improve the results using the *PL* was demonstrated. Concludingly, the presented methodology is shown to facilitate detection of relevant differences between dynamical models of cell types, which is an

important step towards discovering drug targets specifically affecting cells of interest.

References

Akaike,H. (1974) A new look at the statistical model identification. *IEEE Trans. Automat. Control*, **19**, 716–723.

Bachmann,J. *et al.* (2011) Division of labor by dual feedback regulators controls JAK2/STAT5 signaling over broad ligand range. *Molecular Systems Biology*, **7**,

Barrodale,I. and Roberts,F.D.K. (1973) An improved algorithm for discrete L_1 linear approximation. *SIAM J. Num. Anal.*, **10**, 839–848.

Becker,V. *et al.* (2010) Covering a broad dynamic range: Information processing at the erythropoietin receptor. *Science*, **328**, 1404–1408.

Beer,R. *et al.* (2014) Creating functional engineered variants of the single-module non-ribosomal peptide synthetase IndC by T domain exchange. *Mol. BioSyst.*, **10**, 1709–1718.

Box,G.E.P. and Hill,W.J. (1967) Discrimination among mechanistic models. *Technometrics*, **9**, 57–71.

Candes,E.J. and Wakin,M.B. (2008) An introduction to compressive sampling. *IEEE Sign. Process. Magaz.*, **25**, 21–30.

Cheng,H. (2015). The fundamentals of Compressed Sensing. In: *Sparse Representation, Modeling and Learning in Visual Recognition: Theory, Algorithms and Applications*. Springer London, London, pp. 21–53.

Claerbout,J.F. and Muir,F. (1973) Robust modeling with erratic data. *Geophysics*, **38**, 826–844.

Coleman,T. and Li,Y. (1996) An interior, trust region approach for nonlinear minimization subject to bounds. *SIAM J. Optim.*, **6**, 418–445.

Efron,B. *et al.* (2004) Least angle regression. *Ann. Stat.*, **32**, 407–499.

Efroymson,M.A. (1960). *Multiple Regression Analysis. Mathematical Methods for Digital Computers*. John Wiley, New York.

Friedman,J. *et al.* (2007) Pathwise coordinate optimization. *Ann. Appl. Stat.*, **1**, 302–332.

Hocking,R.R. and Leslie,R.N. (1967) Selection of the best subset in regression analysis. *Technometrics*, **9**, 531–540.

Hothorn,T. and Bühlmann,P. (2006) Model-based boosting in high dimensions. *Bioinformatics*, **22**, 2828–2829.

Kabán,A. (2007) On bayesian classification with laplace priors. *Pattern Recogn. Lett.*, **28**, 1271–1282.

Kreutz,C. *et al.* (2012) Likelihood based observability analysis and confidence intervals for predictions of dynamic models. *BMC Syst. Biol.*, **6**, 120.

Levy,S. and Fullagar,P.K. (1981) Reconstruction of a sparse spike train from a portion of its spectrum and application to high-resolution deconvolution. *Geophysics*, **46**, 1235–1243.

Meyer,P. *et al.* (2014) Network topology and parameter estimation: from experimental design methods to gene regulatory network kinetics using a community based approach. *BMC Syst. Biol.*, **8**, 1–18.

Ming Yuan,Y.L. (2006) Model selection and estimation in regression with grouped variables. *J. R Stat. Soc., Ser B*, **68**, 49–67.

Oldenburg,D.W. *et al.* (1983) Recovery of the acoustic impedance from reflection seismograms. *Geophysics*, **48**, 1318–1337.

Raue,A. *et al.* (2009) Structural and practical identifiability analysis of partially observed dynamical models by exploiting the profile likelihood. *Bioinformatics*, **25**, 1923–1929.

Raue,A. *et al.* (2013) Lessons learned from quantitative dynamical modeling in systems biology. *PLoS One*, **8**, e74335.

Raue,A. *et al.* (2015) Data2dynamics: a modeling environment tailored to parameter estimation in dynamical systems. *Bioinformatics*, **31**, 3558–3560.

Schmidt,M. *et al.* (2009) Optimization methods for L_1-regularization. *UBC Technical Report*.

Schwarz,G. (1978) Estimating the dimension of a model. *Ann. Stat.*, **6**, 461–464.

Steiert,B. *et al.* (2012) Experimental design for parameter estimation of gene regulatory networks. *PLoS One*, **7**, 1–11.

Taylor,H.L. *et al.* (1979) Deconvolution with the L_1 norm. *Geophysics*, **44**, 39–52.

Thompson,M.L. (1978) Selection of variables in multiple regression: Part I. a review and evaluation. *Int. Stat. Rev.*, **46**, 1–19.

Tibshirani,R. (1996) Regression shrinkage and selection via the LASSO. *J. R Stat. Soc. Ser. B*, **58**, 267–288.

Tibshirani,R. (1997) The LASSO method for variable selection in the cox model. *Stat. Med.*, **16**, 385–395.

Tibshirani,R. *et al.* (2005) Sparsity and smoothness via the fused LASSO. *Journal of the Royal Statistical Society, Series B*, **67**, 91–108.

Tibshirani,R.J. and Taylor,J. (2011) The solution path of the generalized LASSO. *Ann. Stat.*, **39**, 1335–1371.

Vidaurre,D. *et al.* (2013) A survey of L_1 regression. *Int. Stat. Rev.*, **81**, 361–387.

Wilks,S.S. (1938) The large-sample distribution of the likelihood ratio for testing composite hypotheses. *Ann. Math. Stat.*, **9**, 60–62.

Witten,D.M. and Tibshirani,R. (2010) A framework for feature selection in clustering. *J. Am. Stat. Assoc.*, **105**, 713–726.

Zou,H. and Hastie,T. (2005) Regularization and variable selection via the elastic net. *J. R Stat. Soc. Ser. B*, **67**, 301–320.